Dynamic current activity measurement for integrated circuit emission model

M. Emin Başak, Ayten Kuntman

Istanbul University, Faculty of Engineering, Department of Electrical & Electronics Engineering, 34850, Avcılar, Istanbul, Turkey
mebasak@istanbul.edu.tr, akuntman@istanbul.edu.tr

Abstract

This paper describes the current activity measurement and modeling of integrated circuits for electromagnetic conducted emission. In this study, a test circuit including the MC9S12XMAG-family microcontroller was designed and measurements were made to confirm the applied measurement techniques. Moreover, internal current was obtained from the measured external current which is described as a dynamic current activity on the die. The input impedance measurements were performed in the frequency range from 1MHz to 2GHz. The passive distribution network was extracted with the differential evolution algorithm from the measured impedance – frequency curve and results were compared with the measurements. The external current was measured by the spectrum analyzer has been used to obtain the internal current of the die. Extracted passive distribution network and internal activity component values have been given to obtain the integrated circuit emission model.

1. Introduction

Electromagnetic compatibility (EMC) is the ability of an electrical or electronic product or system can operate accurately in the intended environment without degradation of performance due to unintentional electromagnetic interactions. Passing every day a new electronic product is entering into our lives. Increasing integration of electronic products and/or systems are becoming more complex nowadays. The power and frequency range electronic devices were increasing and creating a more severe and uncontrollable electromagnetic environment. It is difficult to operate in the intended environment without causing performance degradation due to unintentional electromagnetic effects.

The lately developed integrated circuits (ICs) generated the amount of parasitic emissions due to advances in digital and semiconductor technology, higher clock speeds, more complex circuits, upper dynamic current consumption, and insufficient design methods.

Highest in a number of the EMC related problem concentrated on the external part of the IC, despite the fact that, ICs have important functions in many cases of the electromagnetic compatibility of an electronic system. In this study, internal part of the IC core has been focused on.

EMC is generally checked at the end of the design cycle, before the IC is placed on the printed circuit board. If the emission level is higher than the expected, the design will be done again and this will be caused by loss of time and money. Therefore, a model is needed to predict the EM compliance precisely and swiftly. Various electromagnetic models have been generated to predict the behavior of the ICs in electromagnetic environment [1-14]. Integrated circuit emission model (ICEM) [1- 9] and Linear equivalent circuit and current source (LECCS) model [1, 10] has been used for prediction of electromagnetic emission of ICs. Input/Output buffer information specification (IBIS) has been used for printed circuit board (PCB) analysis is the other emission model [11, 12]. An I/O interface model for integrated circuit (ICIM) model has also been used in board design [1,13].

In our previous study [2], a test circuit containing PIC16F628 was designed and measurements were made to obtain the input impedance of the power supply pin of the microcontroller. In [2], the genetic algorithm was used to obtain the model. In this study, a test circuit containing the MC9S12XMAG-family microcontroller was designed and measurements were made to confirm the applied measurement techniques as defined in Section 2 [1, 2]. The test circuit used in previous work [2] is changed to show that this modelling approach can be approved to any other integrated circuits. Network analyzer was performed using the test circuit measurement and no voltage was applied to the circuit during the measurements. In this way the global impedance of the PCB, conducted path, SMA connector and microcontroller core was obtained. Then, the impedance of the PCB, conductive path between the power supply pin and SMA connector, and SMA connector was removed by the de-embedding technique. Passive distribution network (PDN) was obtained from the measured curve. The differential evolution algorithm used for the modelling and it shows very good agreement with the measurement results. The external current, measured with the spectrum analyzer, was used to obtain the internal activity of the IC core. The effect of the amplifier, which was used to obtain the current measurements, was deleted by the de-embedding technique. Obtained passive distribution network and internal activity (IA) of VddPLL power supply pin is modelled by combining.

2. The passive distribution network measurement and modelling

The integrated circuit emission model's objective is to be proposed electrical modelling for integrated circuit internal activities [1-9]. This model will be used to evaluate electromagnetic behavior and performance of electronic equipment. Three ICEM components are needed to describe an ICEM block which is shown in Fig. 1.

i. The passive distribution network component
ii. The internal activity component
iii. The inter-block coupling component

* *This study was supported by the Istanbul University Scientific Research Projects Unit. Project Numbers: 12813 and 13326.*

The power distribution network is a circuit that consists of resistor, capacitor, and inductor elements. Internal activity is the independent current source or voltage source and inter block coupling provides the coupling impedances between blocks and they can be resistive, capacitive and magnetic [9- 12].

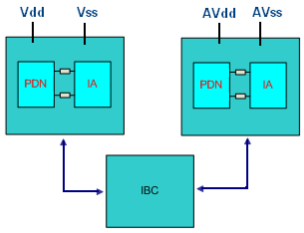

Fig. 1 ICEM block components

The test setup employed to perform such a measurement is shown in Fig. 2. The measurement was achieved placing the coaxial cable directly to SMA connector. Before carrying out the measurement over the component, the **s**hort, **o**pen, **l**oad, and **t**hru (SOLT) calibration method was used to remove the effects of connectors and coaxial cables connected to the network analyzer to the test circuit. The measurement details of the VddPLL –VssPLL (power and ground) pins have been given in this report, owing the fact that all the other supply and ground pins measurement and calculations have been done by the same methodology.

In this study MC9S12XMAG microcontroller, produced by Freescale semiconductor, was used. This 16-bit microcontroller has been widely used in recent automotive electronic systems. Designed and measured MC9S12XMAG microcontroller has been shown in Fig. 3(a) and Fig. 3(b), respectively. This microcontroller fabricated in 0.25 µm CMOS technology. It has eight pairs of power and ground pins to supply the I/O ports, the A/D converter, the oscillator, the phase locked loop (PLL), and the digital core. The pinout of the microcontroller mounted in a thin quad flat patch (TQFP) package with 144 pins.

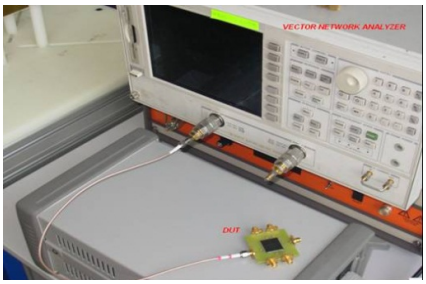

Fig. 2 Measurement configuration of PDN

Because of practical reasons, we measured S parameters; eventually we converted the results to Z parameters. Once the measurements had been done, the impedance model was extracted. It represents a first order resonance, obtaining the global resistance value R at the frequency resonance. But before setting up the impedance model, we should remove the effects of the PCB board, conductive path between the power supply pin and SMA connector, and SMA connector. De-embedding is a mathematical method that removes the undesirable effects of the structure that are embedded in the measured data by deducting their contribution. Traces on the board can cause a larger measured impact than the device under test itself [9].

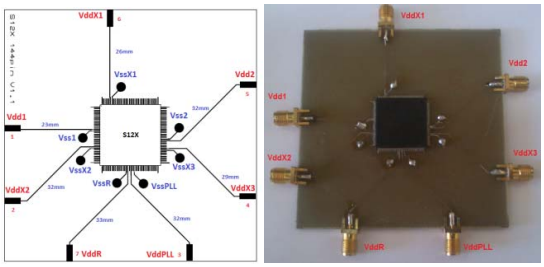

(a) (b)

Fig. 3 (a)Designed and (b) measured MC9S12XMAG microcontroller

S-parameters were measured by network analyzer and then the results translated into impedance Z from which R, L, and C elements were tuned manually. Then, the impedance of the SMA connector, path and board between the power supply pin and SMA connector was deleted by the de-embedding technique. Measured (S_{22}) and de-embedded (S_{11}) input reflection coefficient results are given together in Fig. 4. After measurements of S parameters of the circuits in the specified frequency range were done from 1 MHz to 2 GHz; Z parameters were obtained from S parameters. After all, the passive RLC circuit was extracted again by using the differential evolution algorithm (DEA) is proposed by Storn and Price [14]. The DEA has simple structure and ease of use, in addition to its simple concept. Its very robust algorithm and speed to get the solutions [15]. The main program flowchart of the DEA is shown in Fig. 5. The initial population is comprised of the individuals which are obtained by gene coding. After the obtained the initial population, the function value is computed whether the end condition is satisfied. In this situation individuals are being selected depending on their fitness value. It uses the mutation, crossover, and selection operators which are producing the gather of new solutions. The latter population is more suitable than the former population. In this study the abilities of DEA, such as suitability for simple operation and converging to global optimum, are reflected to extraction of the passive RLC circuit. Each of the R, L, and C component was thought as a chromosome in terms of DEA. The number of repetitions is determined as 200 to obtain the RLC passive elements. During the simulations, new populations represented the new gather of new solutions were produced through crossover and mutation. The RLC circuit was obtained from the measured impedance – frequency curve and the curve which extracted from the model was compared to the measurements.

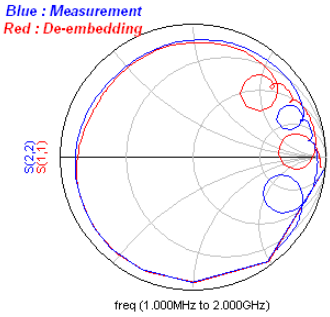

Fig. 4 Measured (S_{22}) and de-embedded (S_{11}) input reflection coefficient results

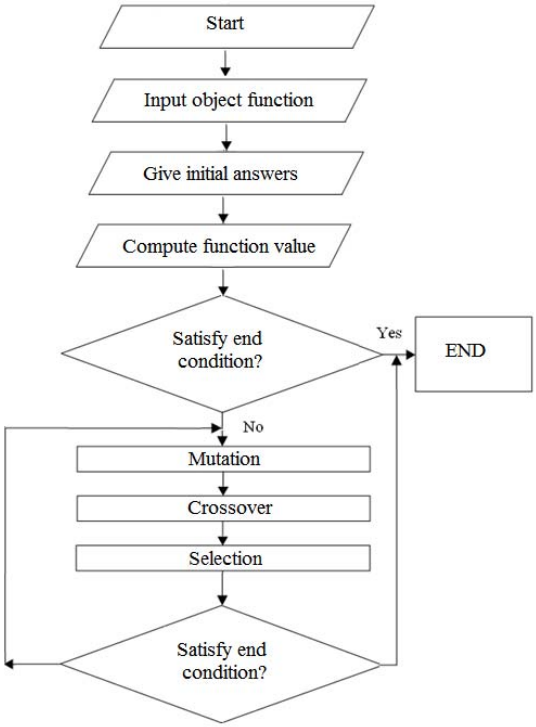

Fig. 5 Main program flowchart of differential evolution algorithm

According to the impedance –frequency curve in Fig. 6 the passive distribution model of the VddPLL power supply pin was extracted by using the DEA. Each R, L and C are assumed as a chromosome. The mutation, crossover, and selection operators have been performed. Fig. 7 represents the RLC model of the power distribution network for the VddPLL power supply pin. It was extracted by using the differential evolution algorithm and the Equations 1-3. Fig. 8 and Fig. 9 represents the correlation between the measurement and the model. The fitness function is the difference between measured and modeled impedance value of the different frequencies.

$$Z_R = R \quad (1)$$

$$Z_C = \frac{1}{j\omega C} \quad (2)$$

$$Z_L = j\omega L \quad (3)$$

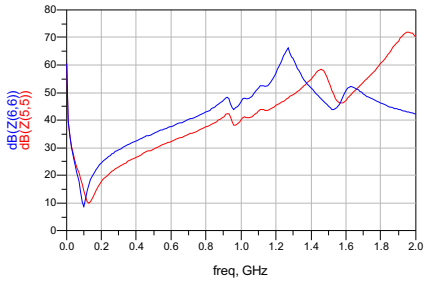

Fig. 6 The new impedance curve obtained by de-embedding operation, the measurement (red line), after removing the effects (blue line)

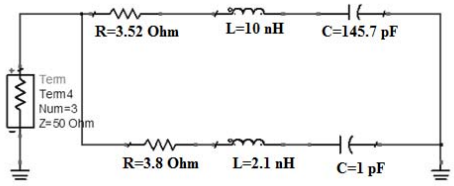

Fig. 7 Passive circuit model of the VddPLL power supply pin

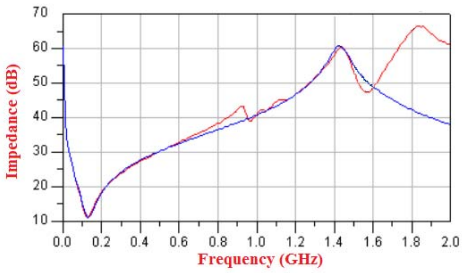

Fig. 8 Correlation between the measurement (red line) and the model (blue line)

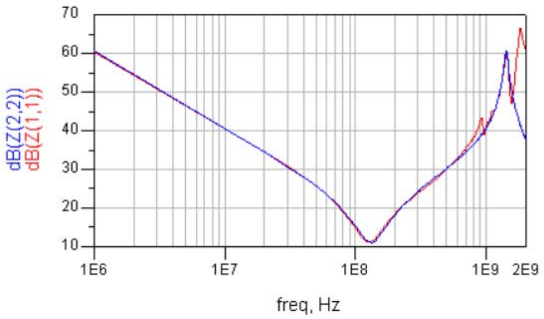

Fig. 9 Correlation between the measurement (red line) and the model (blue line)

3. Internal activity measurement

Most of the time, internal activity (IA) is not accessible directly. The transfer function of PDN has been already extracted and the current flowing externally, I_{ext} has been measured. Depending on which analysis is needed, IA can be described either in the time or in the frequency domain. The current measurement set-up has been used in our measurement shown in Fig. 10. Spectrum Analyzer, power supply, amplifier , and S12X microcontroller were set up in this measurement. Firstly the current, which was used for finding the external current, had been measured.

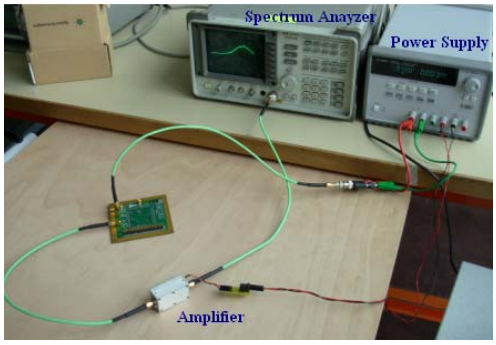

Fig. 10 Measurement configuration of internal activity

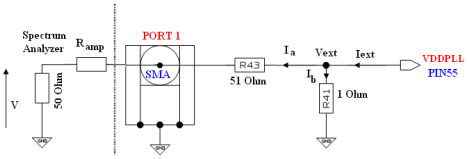

Fig. 11 Measurement of the external current for VddPLL power supply pin

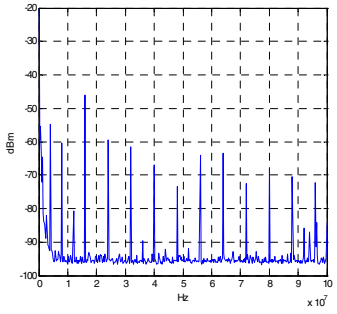

Fig. 12 The measurement result of the external current from 1 MHz to 100 MHz

The current was measured by spectrum analyzer was used to obtain the external current is shown in Fig. 12. After the measurement, the results were calibrated by subtracting the effect of the amplifier. The effect of the amplifier was found by vector network analyzer. Table 1 shows that the measurement results of the amplifier (**Measured P_{dBm}**) and how much the current was amplified (**Amplified P_{dBm}**). After this value had been subtracted from the measured value, the calibrated power (**Calibrated P_{dBm}**) was obtained. Obtaining the real external current of the circuit we also need the value of the amplifier's input impedance (**R_{amp}**). The values of the input impedances of the amplifier were measured by network analyzer and given in Table 1 (**R_{amp} (Ohm)**). The external voltage of the circuit (V_{ext}) was calculated by Equations 4-6 expressing how those values were obtained.

$$P = 10^{\frac{PdBm-30}{10}} \quad (4)$$

$$V = \sqrt{2 \times P \times R} \quad (5)$$

$$V_{ext} = \frac{V}{51 + R_{amp}} + \frac{V}{50} \quad (6)$$

After finding the external current of the circuit (**I_{ext}(mA)**) the internal current was obtained by using PDN and external current as seen in Equation 7. Internal activity is represented in Figure 13 as an ideal current source in parallel with a capacitor. Internal activity current values (**I_{int}(mA)**) are presented in Table 1 for different frequencies.

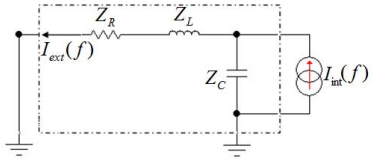

Fig. 13 Finding an internal current

$$I_{\text{int}}(f) = I_{ext}(f) \times \frac{Z_L + Z_C + Z_R}{Z_C} \quad (7)$$

Obtained passive distribution network and internal activity (IA) of VddPLL power supply pin is modelled by combining in Figure 14.

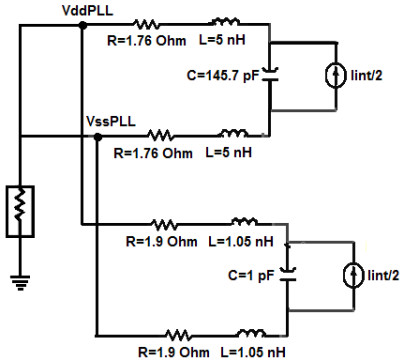

Fig. 14 Obtained model of PDN and internal activity of a VddPLL power supply pin

Table 1 External and internal current values

f (MHz)	1.32	3.9975	16.0127	24.021	32.036	40.071	64.071	96.49
Measured P_{dBm}	-64.10	-55.10	-47.10	-60.17	-61.83	-67.60	-63.50	-69.50
Amplified P_{dBm}	36.94	36.93	36.95	36.93	36.937	36.95	36.95	36.99
Calibrated P_{dBm}	-101.04	-92.03	-84.05	-97.1	-96.76	-104.55	-100.45	-106.49
R_{amp} (Ohm)	85.780	87.776	87.072	85.881	84.466	79.743	74.819	67.245
I_{ext}(mA)	0.01	0.03	0.075	0.016	0.017	0.0068	0.01	0.005
I_{int}(mA)	0.01	0.030	0.079	0.017	0.019	0.046	0.014	0.0096

4. Discussions

In this paper, the power supply conducted emissions of an IC have been evaluated. The power distribution network is characterized by self and transfer impedances. Good agreement between measured and simulated impedances was found. Extracted PDN and IA component values have been given to obtain the integrated circuit emission model. This model will be used to evaluate electromagnetic behavior and performance of electronic equipment. In the future, the exact model will be designed and model results will be compared with the near field measurements for specified frequencies.

5. References

[1] S. B. Dhia, M. Ramdani, E. Sicard, "Electromagnetic compatibility of integrated circuits—techniques for low emission and susceptibility", New York, NY, USA: Springer-Verlag, 2006.

[2] M. E. Başak , A. Kuntman "Tümdevrelerin Elektromanyetik Performansı için Pasif Devre Tasarımı", ELECO 2012, Elektrik Elektronik Bilgisayar Mühendisliği Semp, 29 Kasım -1 Aralık 2012, Bursa.

[3] L. D. Smith, R. E. Anderson, D. W. Forehand, T. J. Pelc, T. Roy, "Power distribution design methodology and capacitor selection for modern CMOS technology", IEEE Trans Adv Packag 1999; 22: 284–291.

[4] J. L. Levant , C. H. Marot , M. Meyer, M. Ramdani, "Solving ASIC decoupling with the ICEM-CE Model", EMC Compo 2009, Toulouse, France

[5] C. Lochot, S. Calvet, S. B. Dhia, E. Sicard, "Regina test masks: Research on EMC guidelines for integrated automotive circuits", Microelectronics J. 2004; 35: 509–524.

[6] K. Slattery, Muccioli JP, North T. Characterization of the RF emissions from a family of microprocessors using a 1 GHz TEM cell. IEEE EMC Symp; 18-22 August 1997; Austin, Texas, TX, USA: 203–207.

[7] T. Steinecke, "Design-in for EMC on CMOS large scale integrated circuits", IEEE Int Symp EMC 2001; 2: 910–915.

[6] B. Vrignon, S. B. Dhia, E. Lamoureux, E. Sicard, "Characterization and modeling of parasitic emission in deep submicron CMOS", IEEE Trans Electromagn Compat 2005; 47: 382–385.

[7] M. Swaminathan, J. Kim, I. Novak, J. P. Libous, "Power distribution networks for system-on-package: status and challenges", IEEE Trans Adv Packag 2004; 27: 286–300.

[8]H. H. Chen, J. S. Neely, "Interconnect and circuit modeling techniques for full-chip power supply noise analysis", IEEE Trans Compon Packag Manuf Technol B 1998; 21: 209–215.

[9] M. Foissac, J. L. Schanen, C. Vollaire, "Black box EMC model for power electronics converter", Energy Conversion Congress and Expo; 20-24 September 2009; San José, United States.

[10] K. Ichikawa, M. Inagaki, and Y. Sakurai, "Simulation of integrated circuit immunity with LEECS model", Proc. 17th Int. Zurich Symp Electromagn Compat, 2006; 308–311.

[11] F. Peivand, Y. Chen, J. Fang, "Extraction of transient behavioral model of digital I/O buffers from IBIS", 46th IEEE Electronic Components and Technology conference 1996; Orlando: 1009-1015.

[12] Y. Wang, H. N. Han Ngee Tan, "The development of analog SPICE behavioral model based on IBIS model", proceedings of the Ninth Great Lakes Symposium on VLSI 1999, 101- 104

[13] K. Nakamura, K. Eguchi, S Hojo, H. Fukuda, "Development of processor for the I/O interface model for integrated circuit (IMIC, EIAJ ED-5302)", DA Symposium 2004; 163-168.

[14] R. Storn and K. Price, "Differential evolution-a simple and efficient heuristic for global optimization over continuous space", Journal of Global Optimization. Volume 11, Number 4, 341-359, 1997 DOI: 10.1023/A:1008202821328

[15] D. G. Mayer, B.P. Kinghorn, A. A. Archer "Differential Evolution – An Easy and Efficient Evolutionary Algorithm for Model Optimisation", Agricultural Systems, Volume 83, Issue 3, March 2005, Pages 315-328